Contribution from the Department of Chemistry,
University of Leuven, Celestijnenlaan 200F, 3030 Heverlee, Belgium

Ligand Field Spectrum and the Electronic Structure of the $Cr(CN)_6^{3-}$ Ion

L. G. VANQUICKENBORNE,* L. HASPESLAGH, M. HENDRICKX, and J. VERHULST

Received August 1, 1983

Ab initio SCF calculations have been carried out for the $Cr(CN)_6^{3-}$ complex in its ground state, for a selected set of ligand field excited states, and for the average of ligand field states $Av(d^3)$. The frozen orbitals of $Av(d^3)$ can be used to calculate all the relevant states with *one* appropriate set of orbitals; this approach offers a convenient meeting point between the Hartree–Fock results proper and simple models such as crystal field theory. Numerically, the SCF results are only moderately successful: they generally reproduce the different excited states in the correct energy range, but quantitatively, certain excitation energies are up to 60% in error. Conceptually, the SCF calculations confirm certain approximations of crystal field theory, but the interpretation of the typical *B*, *C*, and *Dq* parameters are radically different from the classical interpretations.

Introduction

The experimental absorption spectrum of $Cr(CN)_6^{3-}$ is very well-known, both in solution and in the solid state.[1-8] The ligand field bands have been analyzed at three different levels of approximation: crystal field theory,[8] extended Hückel theory,[4] and Xα–MO theory.[10] Since the latter two treatments[4,10] are essentially confined to the calculation of the 10*Dq* parameter, we will focus our attention on the more complete crystal field analysis.

Table I shows the assignments proposed by Witzke,[8] based on a purely octahedral symmetry. The t_{2g}^3 configuration gives rise to four different states, separated by multiples of the Racah parameters *B* and *C*; the ground state is predicted to be the nondegenerate $^4A_2$ state. The ^2E and $^2T_1$ states are degenerate to first order in perturbation theory. This degeneracy can be traced back to the special rotational properties of purely atomic t_{2g} orbitals ($t_{2g}^n - p^n$ isomorphism[11]). It is removed by the higher order interactions between t_{2g}^3 and $t_{2g}^2e_g^1$, leading to a small but detectable energy splitting of 610 cm^{-1}. Two more intense spectral bands are assigned to spin-allowed transitions of the $t_{2g} \rightarrow e_g$ type; one of them, the $^4A_2 \rightarrow {}^4T_{2g}$ transition, corresponds exactly to 10*Dq*. As shown in Table I, the five observed spectral bands can be reproduced quite satisfactorily by a semiempirical fitting of the three crystal field parameters 10*Dq*, *B*, and *C*. The numerical values of the three parameters are in the expected range, and—as a whole—the identification of the ligand field bands in Table I appears to be quite reasonable.

In the present paper, we report the first detailed ab initio calculation[9] of the ligand field spectrum of $Cr(CN)_6^{3-}$. It is our purpose (i) to find out to what extent a large basis set Hartree–Fock calculation is able to reproduce the experimental dd spectrum for a typical strong-field complex and (ii) to gain additional insight into the nature of the approximations made by crystal field theory.

Method of Calculation

We adopted Roothaan's restricted Hartree–Fock method, as applied to open shells in its two-Hamiltonian formalism (η orbitals).[12] In order to increase the rather limited applicability of Roothaan's original method, we used a slight generalization of the formalism by averaging the appropriate *J* and *K* integrals, whenever the energy expression did not have the required symmetry. In this way, the proper degeneracy could always be conserved, while at the same time obtaining the correct energy. This procedure yields exactly the same results as Roothaan's original proposal in those cases, where both methods can be applied—but the present procedure has a much wider range of applicability. In the evaluation of the integrals and the diagonalization of the matrices, maximal advantage was taken of the molecular symmetry.[13] The geometry of the $Cr(CN)_6^{3-}$ ion was taken to be perfectly octahedral with the Cr–C and C–N bond distances at 2.077 and 1.136 Å, respectively.[14-18] The calculations were carried out for the isolated molecular ion, neglecting the influence of the crystalline (or solvent) environment.

For the chromium ion, we used a rather large (15s 11p 6d/12s 8p 4d) GTO basis, as detailed in a previous paper;[19] for the ligand atoms, we used the (9s 5 p/5s 3 p) bases proposed by Huzinaga and Dunning.[20] The combination of these two sets should constitute a well-balanced basis since the absolute error per orbital (deviation from the numerical Hartree–Fock result for an isolated atom) is then roughly the same for metal and ligand orbitals.

The Hartree–Fock calculations were performed for the ground state, for a selected set of ligand field excited states, and for the average of ligand field states of the complex[21-23] (i.e., the average of all the states corresponding to the four configurations t_{2g}^3, $t_{2g}^2e_g^1$, $t_{2g}^1e_g^2$, and e_g^3). The latter calculation is denoted $Av(d^3)$ for $Av(t^{9/5}e^{6/5})$. By using the orbitals of $Av(d^3)$, one can calculate (albeit not so accurately) all the relevant states with one appropriate set of orbitals; this frozen-orbital approach should constitute a convenient meeting point between the Hartree–Fock results and the simple models such as crystal field theory or extended Hückel theory. Indeed, all these simple models use only *one* orbital set of the ground state and for all the excited states; on the other hand, the frozen-orbital calculations should also have a close relationship to the individual SCF-state calculations, having their roots in the same Hartree–Fock formalism and being

(1) H. Kuroya and R. Tsuchida, *Nippon Kaguku Kaishi (1921-47)*, **61**, 597 (1940).
(2) S. Kida, J. Fujita, K. Nakamoto, and R. Tsuchida, *Bull. Chem. Soc. Jpn.*, **31**, 79 (1958).
(3) R. Krishnamurthy and W. B. Schaap, *Inorg. Chem.*, **2**, 605 (1963); R. Krishnamurthy, W. B. Schaap, and J. R. Perumareddi, *ibid.*, **6**, 1338 (1967).
(4) J. J. Alexander and H. B. Gray, *J. Am. Chem. Soc.*, **90**, 4260 (1968).
(5) R. A. Condrate and L. S. Forster, *J. Chem. Phys.*, **48**, 1514 (1968).
(6) R. K. Mukherjee, S. C. Bera, A. Bose, and M. Chowdbury, *J. Chem. Phys.*, **56**, 3720 (1972).
(7) H. Gaussman and H. L. Schläfer, *J. Chem. Phys.*, **48**, 4056 (1968).
(8) H. Witzke, *Theor. Chim. Acta*, **20**, 171 (1971).
(9) An ab initio calculation of the ground state of $Cr(CN)_6^{3-}$ has been reported by M. Sano, H. Kashiwagi, and H. Yamatera, *Inorg. Chem.*, **21**, 3837 (1982).
(10) M. Sano, H. Adachi, and H. Yamatera, *Bull. Chem. Soc. Jpn.*, **54**, 2898 (1981).
(11) J. S. Griffith, "The Theory of Transition Metal Ions", Cambridge University Press, London, 1971.
(12) C. C. J. Roothaan, *Rev. Mod. Phys.*, **32**, 179 (1960).
(13) SYMOL set of programs, as developed by G. A. Van der Velde, Ph.D. Thesis, University of Groningen, The Netherlands, 1974.
(14) W. P. Griffith and G. T. Turner, *J. Chem. Soc. A*, 959 (1970).
(15) J. Jagner, E. Gungström, and N. G. Vannerberg, *Acta Chem. Scand., Ser. A*, **A28**, 623 (1974).
(16) N. G. Vannerberg, *Acta Chem. Scand.*, **26**, 2863 (1972); *ibid.*, **24**, 2335 (1970); *ibid.*, **20**, 1571 (1966).
(17) A. Tullbergh and N. G. Vannerberg, *Acta Chem. Scand.*, **25**, 343 (1971).
(18) R. L. R. Towns and R. A. Levenson, *Inorg. Chem.*, **13**, 105 (1974).
(19) L. G. Vanquickenborne and J. Verhulst, *J. Am. Chem. Soc.*, **105**, 1769 (1983).
(20) T. H. Dunning, *J. Chem. Phys.* **53**, 2823 (1970); S. Huzinaga, *ibid.*, **42**, 1293 (1965).
(21) J. C. Slater, "Quantum Theory of Atomic Structure", Vol. II, McGraw-Hill, New York, 1960.
(22) P. O. D. Offenhartz, *Phys. Rev. B: Solid State*, **B6**, 2876 (1972).
(23) J. W. Richardson, *Phys. Rev. B: Solid State*, **B6**, 2879 (1972).

0020-1669/84/1323-1677$01.50/0

Table I. Assignment of the Experimental Ligand Field Bands of $Cr(CN)_6^{3-}$ after Witzke[8a]

exptl band max	state transition	excited confign	cryst field expressn (first order)	optimal first-order fit (set I)	optimal fit (set II)
12460	$^4A_2 \rightarrow {}^2E$	t_{2g}^3	$9B + 3C$	11499	12312
13070	$^4A_2 \rightarrow {}^2T_1$	t_{2g}^3	$9B + 3C$	11499	12679
18370	$^4A_2 \rightarrow {}^2T_2$	t_{2g}^3	$15B + 5C$	19165	19497
26700	$^4A_2 \rightarrow {}^4T_2$	$t_{2g}^2e_g^1$	$10Dq$	26700	26700
32680	$^4A_2 \rightarrow {}^4T_1$	$t_{2g}^2e_g^1$	$10Dq + 12B$	32676	32679

[a] Two different sets of semiempirical parameters were used to reproduce the spectrum. Set I is based on the first-order crystal field expressions: $B = 498$, $C = 2339$, $Dq = 2670$ cm^{-1}. Set II is based on the complete interaction matrix of all ligand field states: $B = 537$, $C = 2690$, $Dq = 2670$ cm^{-1}. All band positions are in cm^{-1}.

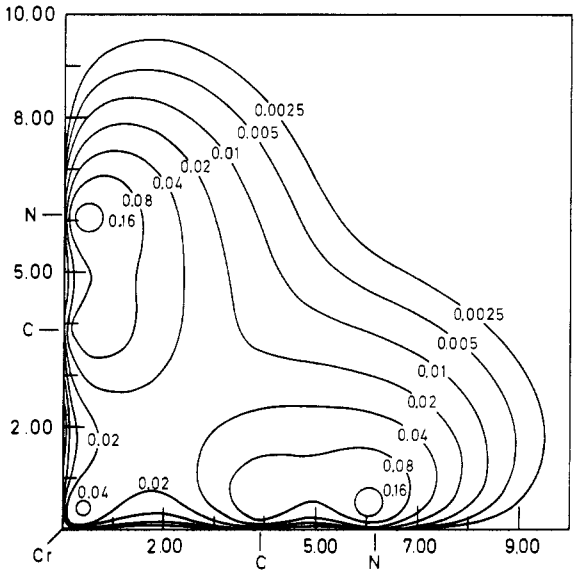

Figure 1. Contours of the $1t_{2g}$ orbital of the Av(d^3) calculation in a plane, containing two bond axes. The coordination axes are graduated in atomic units; the values of the wave functions are in au$^{-3/2}$.

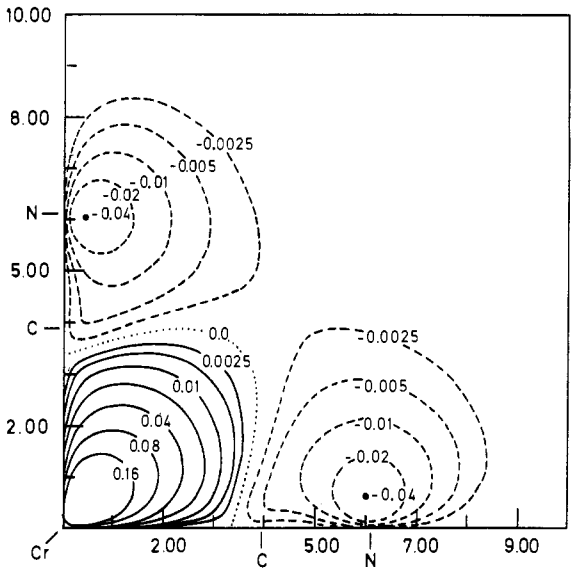

Figure 2. Contours of the $2t_{2g}$ orbital of the Av(d^3) calculation in a plane containing two bond axes. The coordination axes are graduated in atomic units; the values of the wave function are in au$^{-3/2}$.

based on a very similar Hamiltonian.[24]

General Features of the Av(d^3) Calculation

The total energy obtained for the Av(d^3) calculation was −1596.76591 Hartree, reflecting the rather high quality of the basis set.[9] Table II shows the orbital energies and their components for all the occupied orbitals; the last column contains qualitative indications on the nature of the MO's, obtainable from the LCAO coefficients or from a population analysis.

When these results are compared with the classical picture offered by ligand field theory, the following points should be stressed:

(1) All orbitals—without exception—fall into one of two categories: they are predominantly metal centered (metal character greater than 85%) or they are predominantly ligand centered (metal character smaller than 17%) with nothing in between. This result follows from a population analysis, but it finds additional support by a component analysis of the orbital energy. Indeed, all the orbitals with predominant ligand character have an interelectronic repulsion (c_i in Table II) on the order of 20 Hartree, whereas the orbitals with metal character—being significantly more localized—have c_i greater than 35 Hartree. Also the kinetic energy of the metal valence orbitals is 3–5 times larger than the kinetic energy of the ligand-centered valence orbitals; similar trends are observed for the I_i terms. This very clear-cut distinction between two sets of orbitals to some extent supports the basic postulate of crystal field theory, where the complex is described as a perturbed metal ion and where the ligand orbitals are not explicitly considered.

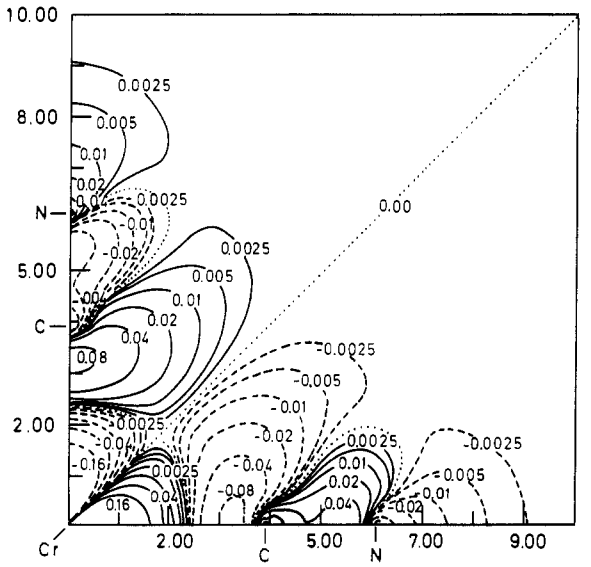

Figure 3. Contours of a $6e_g$ orbital ($d_{x^2-y^2}$ component) of the Av(d^3) calculation in the xy plane (where the two coordinate axes contain two CN ligands). The coordinate axes are graduated in atomic units; the values of the wave functions are in au$^{-3/2}$.

(2) The open-shell orbitals $2t_{2g}$ and $6e_g$ are essentially metal centered as they have 99% and 85% chromium 3d character, respectively. The π orbitals $1t_{2g}$ and $2t_{2g}$ are shown in Figures 1 and 2; they are clearly compatible with the classical idea of a bonding ($1t_{2g}$) and an antibonding ($2t_{2g}$) pair of MO's.

(24) L. G. Vanquickenborne and L. Haspeslagh, *Inorg. Chem.*, **21**, 2448 (1982).

Table II. Energies and Energy Components for the $Av(d^3) = Av(t^{9/5}e^{6/5})$ Calculation (Hartrees)[a]

i	η_i	l_i	t_i	c_i	dominant character
$1a_{1g}$	−220.270 51	−580.701 45	276.762 22	83.668 72	1s(Cr)
$2a_{1g}$	−26.149 31	−136.394 17	50.067 86	60.177 00	2s(Cr)
$1t_{1u}$	−22.074 64	−134.418 29	48.768 43	63.575 22	2p(Cr)
$1e_g$	−15.154 34	−61.050 90	22.123 68	23.772 88	} 1s(N) = 1σ(CN)
$2t_{1u}$	−15.154 34	−61.050 82	22.123 60	23.772 87	
$3a_{1g}$	−15.154 34	−61.050 88	22.123 65	23.772 88	
$2e_g$	−10.830 26	−52.977 41	16.017 11	26.130 04	} 1s(C) = 2σ(CN)
$3t_{1u}$	−10.830 26	−52.977 22	16.016 94	26.130 03	
$4a_{1g}$	−10.830 25	−52.977 76	16.017 44	26.130 07	
$5a_{1g}$	−3.184 38	−53.287 90	10.322 15	39.781 37	3s(Cr)
$4t_{1u}$	−1.930 24	−50.184 32	8.952 18	39.301 90	3p(Cr)
$6a_{1g}$	−0.839 92	−24.085 32	2.287 19	20.958 21	} 3σ(CN)
$5t_{1u}$	−0.837 33	−24.094 04	2.310 36	20.946 35	
$3e_g$	−0.836 61	−24.097 33	2.315 18	20.945 53	
$7a_{1g}$	−0.302 58	−25.175 73	1.503 80	23.369 34	} 4σ(CN)
$6t_{1u}$	−0.214 78	−22.692 72	1.843 72	20.634 22	
$4e_g$	−0.213 97	−23.614 83	1.949 72	21.451 14	
$8a_{1g}$	−0.148 95	−20.890 01	1.843 39	18.897 67	σ(CN)
$5e_g$	−0.121 27	−24.058 63	1.872 76	22.064 61	σ(CN)
$7t_{1u}$	−0.120 86	−22.355 15	1.588 04	20.646 25	σ,π(CN)
$1t_{2g}$	−0.096 75	−21.380 82	1.238 41	20.045 67	π(CN)
$1t_{2u}$	−0.070 07	−21.244 49	1.342 41	19.832 00	π(CN) } pure ligand
$1t_{1g}$	−0.058 17	−21.241 88	1.400 39	19.783 33	π(CN) }
$8t_{1u}$	−0.054 95	−22.236 82	1.525 88	20.655 99	σ,π(CN)
$2t_{2g}$	−0.152 63	−41.883 77	5.635 11	36.096 03	3dπ(Cr) } open shells
$6e_g$	−0.045 72	−42.093 99	6.239 49	35.808 78	3dσ(Cr) }
$E = -1596.765\ 91$		$L = -5501.485\ 80$	$T = 1599.262\ 03$		$C = 1465.426\ 76$
		$L_c = -5375.582\ 23$	$T_c = 1581.631\ 44$		$C_c = 1359.612\ 88$
		$L_o = -125.903\ 57$	$T_o = 17.630\ 59$		$C_o = 2.129\ 50$
					$C_{oc} = 103.684\ 39$

[a] For the individual orbitals the orbital energy $\eta_i = l_i + t_i + c_i$, where l_i, t_i, and c_i represent the electron attraction to the nuclei, the interelectronic repulsion, and the kinetic energy associated with orbital i. Capital letters L, C, and T refer to the corresponding all-electron quantities: $E = T + V = T + L + C + N$. The subscripts o and c refer to the open and the closed shells, respectively; for instance, $L = L_o + L_c$. The total internuclear repulsion N is 840.031 094 Hartree, and the virial ratio $-V/T = 1.998\ 439$.

A remarkable feature of the $2t_{2g}$ orbital is that the nodal surface between Cr and C is quite close to the carbon nucleus (at ~0.25 Å).

The more covalent nature of the $6e_g$ orbital (85% Cr, 15% CN) is also apparent from Figure 3. The nodal surface, at ~2.3 au from the metal nucleus, is characteristic of the antibonding nature of the $6e_g$ orbital; it is situated more nearly midway between the metal and the ligands.

On the whole, the open shells correspond to the expected picture of slightly antibonding metal-centered orbitals, where the σ interactions are significantly stronger than the π interactions.

(3) The cyanide ligand is a σ donor; as for the π interactions, it is usually considered to have π-donor and (weaker) π-acceptor properties. If we carry out a separate SCF calculation on the CN^- ion (using the same basis set as in the complex), the relevant π orbitals are found to be of the form roughly summarized by

$$\pi(CN^-) \sim 0.62[2p(C)] + 0.78[2p(N)] \quad (1a)$$

$$\pi^*(CN^-) \sim 0.87[2p(C)] - 0.50[2p(N)] \quad (1b)$$

and the $2t_{2g}$ MO of the complex can be approximated as

$$2t_{2g} \sim 0.99[3d(Cr)] + 0.00[2p(C_6)] + 0.14[2p(N_6)] \sim 0.99[3d(Cr)] - 0.12[\pi(CN^-)_6] + 0.09[\pi^*[(CN^-)_6]] \quad (2)$$

where for instance $2p(C_6)$ is the appropriate linear combination of 2p orbitals on the six carbon atoms. Equation 2 suggests that the π-donor and the π-acceptor properties of the cyanide ion are nearly equal in $Cr(CN)_6^{3-}$. The signs of the LCAO coefficients correspond to what could be expected on simple grounds: antibonding (−) combination with $\pi(CN^-)$; bonding (+) combination with $\pi^*(CN^-)$. The very small electron density at the carbon atoms in $2t_{2g}$ is obviously connected to this particular arrangement.

If the ligand were a pure π donor, one would expect a nodal plane between Cr and C and not between C and N; if the ligand were a pure π acceptor, one would expect a nodal plane between C and N and not between Cr and C. Figure 2 suggests that the π-donor properties dominate, albeit only slightly; this is the reason why the nodal plane is so close to the carbon nucleus.

The near-balance between π-donor and π-acceptor properties seems to be confirmed by the considerations of Sano et al.,[10] who report a net dπ population of 2.97 electrons (rather than 3). A more detailed analysis of orbital populations and difference density plots will be published in a subsequent paper.

(4) The orbital energy sequence is not particularly revealing; the fact that the open-shell $2t_{2g}$ MO is a rather deep-lying orbital does not prevent the d–d transitions from having the lowest energy. Orbital energy differences $\Delta\eta$ are not directly or simply related to the corresponding state energy differences ΔE. This fact has been observed and discussed before;[25,26] it hardly affects the ligand field picture of transition-metal complexes. Although the spectrum will be discussed in more detail in the next sections, one additional comment might be useful at this point. If the c_i repulsion terms of Table II are further analyzed, the J_{ii} integrals are found to be on the order of 0.8 Hartree for the metal-centered orbitals vs. 0.2 Hartree for the ligand-centered orbitals. This very large energy difference is one of the reasons why $\Delta\eta$ and ΔE are not even qualitatively similar.

(5) Only two MO's are purely (100%) ligand orbitals: the basis set contains no metal functions of t_{1g} or t_{2u} symmetry. The $1t_{1g}$ and $1t_{2u}$ orbitals are just different linear combinations

(25) J. Demuynck, A. Veillard, and G. Vinot, *Chem. Phys. Lett.*, **10**, 522 (1971).
(26) A. J. H. Wachters and W. C. Nieuwpoort, *Phys. Rev. B: Solid State*, **5**, 4291 (1972).

Table III. Griffith and Racah Parameters as a Function of Certain J and K Integrals[a]

$a = J_{\xi\xi} = J_{\eta\eta} = J_{\zeta\zeta} = J_{tt}$	$A + 4B + 3C$
$b = J_{\xi\eta} = J_{\xi\zeta} = J_{\eta\zeta} = J_{tt'}$	$A - 2B + C$
$j = K_{\xi\eta} = K_{\xi\zeta} = K_{\eta\zeta} = K_{tt'}$	$3B + C$
$e = J_{\theta\theta} = J_{\epsilon\epsilon} = J_{ee}$	$A + 4B + 3C$
$f = K_{\theta\epsilon} = K_{ee'}$	$4B + C$
$c = (3^{1/2}/2)(J_{\theta\xi} - J_{\epsilon\xi}) = (3^{1/2}/2)(J_{\theta\eta} - J_{\epsilon\eta})$	$2B3^{1/2}$
$d = J_{\epsilon\xi} = J_{\epsilon\eta}$	$A - 2B + C$
$g = K_{\theta\xi} = K_{\theta\eta}$	$B + C$
$h = (3^{1/2}/2)(K_{\epsilon\xi} - K_{\theta\xi}) = (3^{1/2}/2)(K_{\epsilon\eta} - K_{\theta\eta})$	$B3^{1/2}$
$K_{ee'} - K_{tt'} = f - j$	B
$K_{\epsilon\zeta}$	C

[a] As usual,[11] θ and ϵ are the two e_g orbitals, transforming like z^2 and $x^2 - y^2$, respectively; ξ, η, and ζ are the three t_{2g} orbitals, transforming like yz, xz, and xy, respectively.

Table IV. Interelectronic Repulsion within the Open Shells as a Function of the Griffith and the Racah Parameters for a Selected Set of States and Averages of States[a]

$^4A_{2g}(t^3)$	$3b - 3j$	$3A - 15B$
$^2E_g(t^3)$	$3b$	$3A - 6B + 3C$
$^2T_{1g}(t^3)$	$a + 2b - 2j$	$3A - 6B + 3C$
$^2T_{2g}(t^3)$	$a + 2b$	$3A + 5C$
$^4T_{2g}(t^2e^1)$	$b + 2d - 2g - (4/3^{1/2})h - j$	$3A - 15B$
$^4T_{1g}(t^2e^1)$	$b + 2d + (4/3^{1/2})c - 2g - j$	$3A - 3B$
$Av(t^3)$	$^3/_5(a + 4b - 2j)$	$3A - 6B + 3C$
$Av(t^2e^1)$	$^1/_5(a + 4b - 2j) + 2d + (2/3^{1/2})c - g - (1/3^{1/2})h$	$3A - 4B + 2C$
$Av(t^1e^2)$	$e - ^5/_3f + 2d + (2/3^{1/2})c - g - (1/3^{1/2})h$	$3A - ^{14}/_3B + ^7/_3C$
$Av(e^3)$	$3e - 5f$	$3A - 8B + 4C$
$Av(d^3)$	$^1/_5(a + 4b - 2j) + ^2/_5(e - ^5/_3f) + ^4/_5(2d + (2/3^{1/2})c - g - (1/3^{1/2})h)$	$3A - ^{14}/_3B + ^7/_3C$

[a] The definitions of the parameters are given in Table III.

of the 12 $\pi(CN^-)$ MO's. Therefore, the energy difference $\eta(1t_{1g}) - \eta(1t_{2u}) = 0.32$ eV is essentially due to interligand interactions.

Ligand Field States in the Frozen-Orbital Approximation

Crystal field theory is one particular form of a frozen-orbital approximation, where the open shell is supposed to be made up of pure 3d orbitals. In that case, the d–d repulsion energies can be parametrized by only three Racah parameters A, B, and C (see also Table I, fourth column). In general, however, if the open shell is allowed to expand toward the ligands, giving rise to molecular orbitals of the type

$$3\tilde{d} = c_1(3d) + c_2\varphi(CN) \qquad (3)$$

one needs 10 parameters in order to describe the $3\tilde{d}$–$3\tilde{d}$ open-shell repulsion[11] (see Table III). The use of these 10 Griffith parameters a, b, c, ..., j is not very practical as there are nearly always less experimental bands than parameters. However, from the present point of view, it is obviously useful to compare the frozen-orbital calculations to the Griffith parameterization scheme. Table IV shows the open-shell repulsion energy expressions for the six observed states and for the appropriate averages. The Racah parameter expression in Table IV can be seen as a particularization of the Griffith expressions for atomic 3d functions. Indeed, in the latter case, the 10 Griffith parameters are no longer independent: $a = e$, $b = d$, $a - b = 2j$, etc.

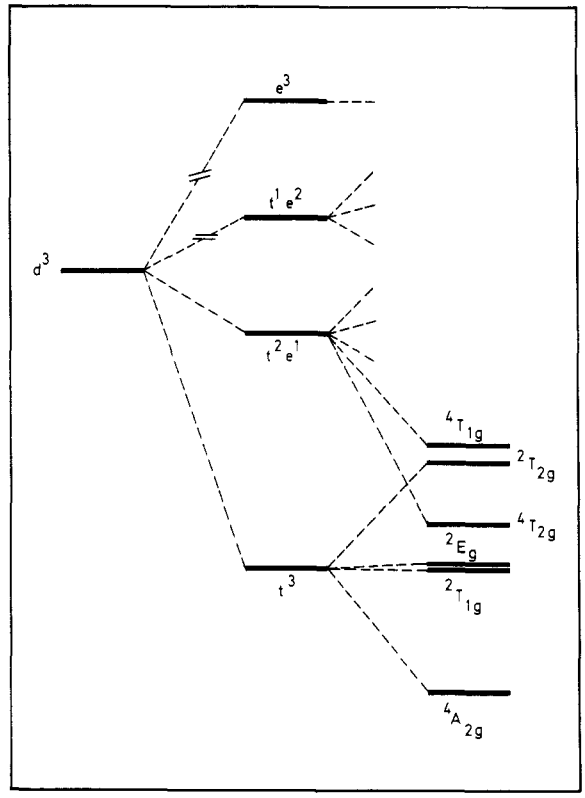

Figure 4. Schematic energy level diagram of the ligand field average (d^3), the four t^xe^{3-x} configuration averages, and a number of relevant states. All energies are calculated by using the frozen eigenvectors of the SCF equations for the $Av(d^3)$ situation.

Figure 4 and Table V show the energy level diagram and the numerical results based on the frozen orbitals of the $Av(d^3)$ SCF calculation.

(1) Within any given configuration, the E differences are equal to the C differences and to the C_o differences. Obviously, the energy differences of Table V are determined by the ex-

Table V. Energy of a Number of Selected States and State Averages, Based on the Frozen Orbitals of $Av(d^3) = Av(t^{9/5}e^{6/5})$[a]

	ΔE	ΔH	ΔC	ΔL	ΔT	ΔC_o	ΔC_{oc}	ΔL_o	ΔT_o
$^4A_{2g}$	0	0	0	0	0	0	0	0	0
$^2T_{1g}$	20 095	0	20 095	0	0	20 095	0	0	0
^2E_g	20 111	0	20 111	0	0	20 111	0	0	0
$^2T_{2g}$	33 502	0	33 502	0	0	33 502	0	0	0
$^4T_{2g}$	22 845	86 507	−63 662	−46 136	132 643	−9 128	−54 534	−46 136	132 643
$^4T_{1g}$	34 191	86 507	−52 316	−46 136	132 643	2 218	−54 534	−46 136	132 643
$Av(t^3)$	20 101	0	20 101	0	0	20 101	0	0	0
$Av(t^2e^1)$	40 501	86 507	−46 006	−46 136	132 643	8 528	−54 534	−46 136	132 643
$Av(t^1e^2)$	63 568	173 014	−109 446	−92 272	265 286	−378	−109 068	−92 272	265 286
$Av(e^3)$	89 301	259 521	−170 219	−138 407	379 928	−6 617	−163 602	−138 407	397 928
$Av(d^3)$	45 647	103 808	−58 161	−55 363	159 171	7 280	−65 441	−55 363	159 171

[a] All energies and energy components (cm^{-1}) are given with respect to the $^4A_{2g}$ ground state. The conversion to the conventional zero of energy can be made by means of Table II. As usual $E = T + V = T + L + C + N = H + C + N$; also $L = L_o + L_c$, etc., where the subscripts o and c refer to the open and closed shells, respectively.

pressions given in Table IV, using the calculated values of the Griffith integrals for Av(d^3).

For the t^3 configuration, ^2E_g and $^2T_{1g}$ are very nearly degenerate (their energy difference is only 18 cm^{-1}). In the purely atomic crystal field theory, both states have exactly the same open-shell repulsion energy, given by $3A - 6B + 3C$. In frozen-orbital MO theory, Table IV shows that their energy difference is given by $a - b - 2j$. The numerical value in Hartree of these integrals is as follows for Av(d^3):

$$a = J_{tt} = 0.790\,34 \qquad b = J_{tt'} = 0.729\,32$$
$$j = K_{tt'} = 0.030\,55 \tag{4}$$

The fact that the energy difference between a–b and $2j$ amounts to only 8×10^{-5} Hartree or 18 cm^{-1} is an additional indication of the nearly pure metal 3d character in the $2t_{2g}$ open shell: for atomic 3d orbitals $J_{tt} - J_{tt'}$ equals exactly $2K_{tt'}$ for symmetry reasons. Since the deviations in the complex are almost negligible, the ligand field spectrum (or at least part of it) can be treated quite satisfactorily as if the open shells were completely metal centered.

In crystal field theory, one has

$$\frac{E(^2E_g,^2T_{1g}) - E(^4A_{2g})}{E(^2T_{2g}) - E(^4A_{2g})} = \frac{9B + 3C}{15B + 5C} = \frac{3}{5} \tag{5}$$

A similar expression can be written in MO theory by taking the weighted average of the open-shell repulsion in ^2E_g and $^2T_{1g}$. If one denotes this average by ^2X and if the subscript o refers to the open shell, one finds

$$C_o(^2X) = \tfrac{2}{5}C_o(^2E_g) + \tfrac{3}{5}C_o(^2T_{1g}) = \tfrac{3}{5}(a + 4b - 2j)$$

and as a consequence

$$\frac{E(^2X) - E(^4A_{2g})}{E(^2T_{2g}) - E(^4A_{2g})} = \frac{\Delta E_a}{\Delta E_b} = \frac{3}{5} \tag{6}$$

Because of eq 4, $E(^2E_g) \simeq E(^2T_{1g}) \simeq E(^2X)$ and, therefore, the ratio 3/5 is found back in the E, C, and C_o columns of Table V.

(2) For an interconfigurational transition, corresponding to a $t_{2g} \rightarrow e_g$ excitation, $\Delta E = \Delta C + \Delta H$, where $\Delta C = \Delta C_o + \Delta C_{oc}$ and $\Delta H = \Delta T + \Delta L$ (the subscripts o refer to the open shells, c to the closed shells, and oc to the interactions between open and closed shells). For the three possible $t_{2g} \rightarrow e_g$ excitations under consideration ($t_{2g}^3 \rightarrow t_{2g}^2e_g^1$, $t_{2g}^2e_g^1 \rightarrow t_{2g}^1e_g^2$, and $t_{2g}^1e_g^2 \rightarrow e_g^3$) H, L, T, and C_{oc} change by a constant amount, given by

$$h(e_g) - h(t_{2g}) = 86\,507\ cm^{-1}$$
$$l(e_g) - l(t_{2g}) = -46\,136\ cm^{-1}$$
$$t(e_g) - t(t_{2g}) = 132\,643\ cm^{-1} \tag{7}$$
$$c_{oc}(e_g) - c_{oc}(t_{2g}) = -54\,534\ cm^{-1}$$

as can be verified from Table V and from Table II.

The open-shell repulsion difference ΔC_o depends on the particular states under consideration. For the $^4A_{2g}(t^3) \rightarrow {}^4T_{2g}(t^2e^1)$ transition, it is given by

$$\Delta C_o = -2b + 2d - 2g - (4/3^{1/2})h + 2j = -9128\ cm^{-1} \tag{8}$$

It is interesting to compare this result to the crystal field expression where the $^4A_{2g} \rightarrow {}^4T_{2g}$ transition is simply given by $10Dq$, since the open-shell repulsion in both studies is identical ($3A - 15B$) and hence $\Delta C_o = 0$ at the crystal field level. In fact, eq 8 shows that, at the frozen MO level, the open-shell repulsion is 9128 cm^{-1} smaller in the excited state. Only when $b = d$ and $j - g = (2/3^{1/2})h$ (the free-ion situation) will eq 8 go to zero. The reason why the discrepancy between the crystal field and the MO picture is much more severe here than for the intra t^3 transitions is directly related to the differential covalency of $2t_{2g}$ and $6e_g$: since the e_g open shell is more covalent than the t_{2g} open shell, the e_g-repulsion integrals deviate more from a free-ion situation than the t_{2g}-repulsion integrals. Since eq 8 contains both pure t_{2g} integrals and mixed e_g–t_{2g} integrals, its deviation from zero is more pronounced.

Table VI. Comparison of the Experimental Absorption Bands and the Frozen-Orbital SCF Calculations of Table V (Energies in cm^{-1})

transition	expt (from Table I)	frozen-orbital calcn (from Table V)	SCF calcn (from Table VII)
$^4A_{2g} \rightarrow {}^2E_g$	12 460	20 111	20 461
$^4A_{2g} \rightarrow {}^2T_{1g}$	13 070	20 095	20 446
$^4A_{2g} \rightarrow {}^2T_{2g}$	18 370	33 502	33 642
$^4A_{2g} \rightarrow {}^4T_{2g}$	26 700	22 845	23 051
$^4A_{2g} \rightarrow {}^4T_{1g}$	32 680	34 191	34 696

In the spirit of crystal field theory it appears reasonable to call $10Dq$ the sum of all those components of $E(^4T_{2g}) - E(^4A_{2g})$ that are not due to ΔC_o:

$$10Dq(FO) = \Delta L + \Delta T + \Delta C_{oc}$$
$$\Delta E = E(^4T_{2g}) - E(^4A_{2g}) =$$
$$10Dq(FO) - 2b + 2d - 2g - (4/3^{1/2})h + 2j \tag{9}$$

where FO stands for frozen orbitals.[27] Numerically, $10Dq$(FO) is found to be 31 973 cm^{-1}, leading to a ΔE value of 22 845 cm^{-1} in eq 9. A comparison of eq 7 and 9 shows that the only positive contribution to $10Dq$(FO) is ΔT.

This is a somewhat curious conclusion, especially in view of the crystal field picture, where one expects $10Dq$ to consist of the supposedly increased repulsion between the d electrons and the ligands. Therefore, crystal field theory suggests a positive contribution of ΔC_{oc} and a ΔT contribution of zero. In order to understand the results of Table V, it is useful to consider the energy components of the open-shell orbitals in Table II. The repulsion (c_i) is seen to be smaller in the $6e_g$ orbital than in $2t_{2g}$ (because of the decreased covalency in $2t_{2g}$), but at the same time, the one-electron energy ($h_i = l_i + t_i$) of $6e_g$ is larger than for $2t_{2g}$; the dominant term is the kinetic energy t_i. The latter fact suggests that the $6e_g$ orbital is more contracted than $2t_{2g}$. This paradoxical conclusion can be reconciled with the enhanced $6e_g$ covalency by a closer inspection of the LCAO coefficients of the open-shell orbitals. Then it appears that the 3d part of the MO's is definitely more contracted for $6e_g$: the coefficients for the two most compact 3d basis functions are larger, and the coefficients for the two most diffuse 3d basis functions are smaller than in $2t_{2g}$. As a result of the more strongly antibonding properties of $6e_g$, the 3d part is more contracted, the orbital as a whole is characterized by regions of larger curvature, and its kinetic energy (Δ operator) is larger.

The picture emerging from these considerations is quite different from the crystal field ideas: the reason why a $t_{2g} \rightarrow e_g$ transition is an energy-demanding process is not due to increased electron–ligand repulsion, but rather to a metal 3d contraction and the corresponding increased orbital curvature.

(3) Table VI shows a comparison of the ΔE values calculated from Table V with the experimental data, taken from Table I. The interconfigurational transitions ($t_{2g} \rightarrow e_g$) are

(27) It has been noted by J. P. Dahl and C. J. Ballhausen, *Adv. Quantum Chem.*, 4, 170 (1968), that $E(^4T_{2g}) - E(^4A_{2g}) = \eta(6e_g;{}^4T_{2g}) - \eta(2t_{2g};{}^4A_{2g})$, where e.g. $\eta(6e_g;{}^4T_{2g})$ is the $6e_g$-orbital energy in the $^4T_{2g}$ state. This equation holds indeed true if one works in a frozen-orbital approximation. However, it is specific for the two states under consideration, and a general equation of the type $\Delta E = \Delta\eta$ is certainly not valid. Therefore, we prefer to work with eq 9.

Table VII. Results of SCF Calculations on the $^4A_{2g}$ Ground State of $Cr(CN)_6^{3-}$ [a]

	closed-shell components	open-shell components	interaction components
$E' = -1596.976\,65$			
$N = 840.031\,09$			
$L' = -5501.740\,11$	$L_c' = -5374.633\,89$	$L_o' = -127.106\,21$	
$T' = 1598.863\,27$	$T_c' = 1581.501\,41$	$T_o' = 17.361\,86$	
$C' = 1465.869\,10$	$C_c' = 1358.883\,26$	$C_o' = 2.152\,95$	$C_{oc}' = 104.832\,87$

[a] The total energy E' and its components are given in Hartrees; T' is the kinetic energy, L' is the electron–nucleus attraction energy, and C' is the interelectronic repulsion component; o refers to the open and c to the closed shells. The primes are used to distinguish the SCF results from the frozen-orbital calculations.

Table VIII. SCF Energy and Its Components for the Six Observed States[a]

	$\Delta E'$	$\Delta H'$	$\Delta C'$	$\Delta L'$	$\Delta T'$	$\Delta C_o'$	$\Delta C_{oc}'$	$\Delta L_o'$	$\Delta T_o'$	$\Delta C_c'$	$\Delta L_c'$	$\Delta T_c'$
$^4A_{2g}$	0	0	0	0	0	0	0	0	0	0	0	0
$^2T_{1g}$	20 446	73 267	−52 821	109 547	−36 280	7 422	−193 941	321 360	−100 738	133 700	−211 815	64 458
^2E_g	20 461	73 648	−53 187	109 896	−36 249	7 376	−194 731	322 222	−100 696	134 169	−212 328	64 444
$^2T_{2g}$	33 642	124 689	−91 047	185 812	−61 124	10 352	−340 800	560 485	−172 118	239 402	−374 675	110 994
$^4T_{2g}$	23 051	90 458	−67 412	−11 085	101 543	−8 474	−45 480	−57 454	134 905	−13 453	46 369	−33 361
$^4T_{1g}$	34 696	98 681	−63 998	18 007	80 674	−4 889	−163 552	141 405	72 782	104 453	−123 400	7 892

[a] All energies are expressed in cm^{-1} and are referred to the $^4A_{2g}$ ground state as zero point. The conversion to the conventional zero of energy can be made by using the results of Table VII. The primed symbols have the same meaning as the corresponding unprimed (frozen-orbital) symbols in Table V.

rather well reproduced, although the ΔE value is apparently somewhat too small. For the intraconfigurational $t^3 \rightarrow t^3$ transitions on the other hand, the calculated values are too high: the experimental numbers are only about 60% of the calculated numbers. The fact that the order of the ^2E_g and the $^2T_{1g}$ states is not correctly reproduced is inherent to the Hartree–Fock level of approximation; as stressed already in the Introduction, the somewhat lower position of ^2E is due to configuration interaction effects, especially with the $2E(t_{2g}^2e_g^1)$ state.

SCF Calculations for the Individual States

Table VII shows the total SCF energy E' and its components for the $^4A_{2g}$ ground state. Table VIII shows the energy differences between ground and ligand field excited states. For the SCF energy and its components, we use primed symbols in order to stress the distinction with the frozen-orbital calculations. The difference between Tables V and VIII reflects the relaxation effects accompanying the transition from the frozen-orbital approximation to the complete SCF calculations. In the latter case, the orbitals are modified so as to minimize the energy of the specific state under consideration, and not just the average d^3 situation. In Table VIII, every state is characterized by its own optimized orbitals.

As could be expected from previous work,[23,24,28] the total relaxation energies $\Delta E' - \Delta E$ are almost negligibly small (of the order of a few hundred cm^{-1}). Therefore, as far as total energies are concerned (the only readily observable quantities), the frozen-orbital calculations are nearly as good (or as bad) as the ΔSCF calculations.

However, the relaxation effect on the energy components is seen to be dramatical. The most striking result is that $\Delta C'$ is *negative* for the three intraconfigurational (t^3) transitions, whereas the corresponding ΔC are positive. So, whereas the frozen-orbital calculation (and ligand field theory) situate the t^3 doublets at higher energy *only* because of higher interelectronic repulsion, the SCF results reveal that the repulsion *decreases* with higher E':

$$C'(^4A_{2g}) > C'(^2T_1) > C'(^2E_g) > C'(^2T_{2g}) \qquad (10)$$

The reason why the doublets are higher in energy than the ground state apparently lies in the *one-electron terms*, especially in the electron–nucleus attraction contribution.

These observations are reminiscent of the situation in isolated metal atoms or ions, where exactly the same inequalities have been reported.[24] As discussed in ref 24, it is quite probable that these results are not an artifact of the SCF solutions but that they are valid for the exact solutions as well. The similarity between eq 10 and the corresponding inequalities in free ions is an alternative manifestation of the fact that the Cr^{3+} ion behaves—at least to some extent—as a separated entity within the $Cr(CN)_6^{3-}$ complex.

The nature of the relaxation process in an intraconfigurational transition can be rationalized in the following way: let us start off from the $^4A_{2g}$ ground state in its SCF description of Table VII. If the frozen orbitals of this ground state were used to describe the excited states, the t_{2g}^3 doublets would be found at $\Delta E = \Delta C = \Delta C_o$ above the ground state, whereas $\Delta L = \Delta T = 0$. Since the original orbitals were derived to minimize the $^4A_{2g}$ energy, they will not be strictly optimal for the excited doublets. The fact that ΔC_o has been increased without changing ΔT and/or ΔL clearly violates the virial theorem, and the balance between L, T, and C has to be restored by a change in the orbital shape. As was already shown for free metal ions, the relaxation will always tend to oppose the originally induced change (here $\Delta C_o > 0$). This can be accomplished by expanding the open-shell orbitals; the subsequent decrease of nuclear screening causes the core orbitals to contract. As a consequence, C_c and T_c increase, while C_o, C_{oc}, and T_o decrease; the electron–nucleus attraction terms L, being negative, exhibit the opposite behavior.

This is precisely the evolution obtained from a comparison of Tables V and VIII. The prime mover of the relaxation process, the C_o increase, entails the whole series of component shifts shown in Figure 5. It is well to stress that $\Delta C_o'$ remains positive in Table VIII, albeit reduced by a factor of about 3. The dominant contribution to $\Delta C'$ (making it negative) is seen to be $\Delta C_{oc}'$: the expansion of the open-shell valence orbitals and the contraction of the closed-shell core induces a very large decrease in C_{oc}'. As a net consequence the relaxation overcompensates the original change in C, decreasing C' rather than increasing it. It is also evident from the table that the magnitude of the individual component shifts can be quite impressive (up to 500 000 cm^{-1}) whereas the total relaxation energy in all cases amounts to practically zero. This is of course related to the fact that the variational principle—for arbitrary orbital changes $\delta\varphi$—guarantees the vanishing of δE, but not of any of its components.[29]

(28) T. F. Soules, J. W. Richardson, and D. M. Vaught, *Phys. Rev. B: Solid State*, 3, 2186 (1971).

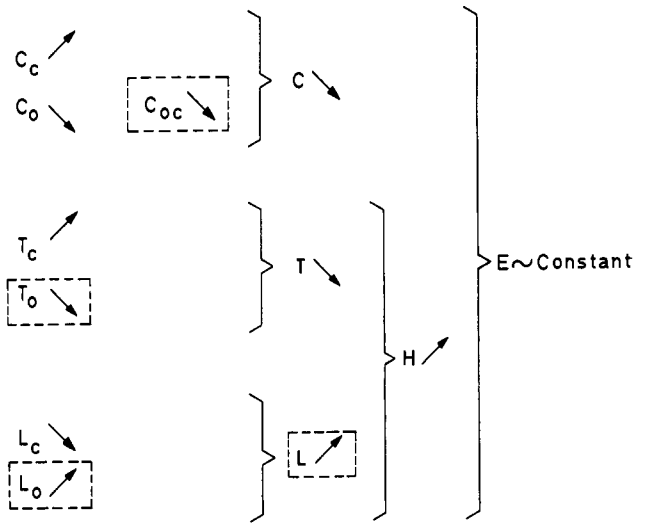

Figure 5. Direction of the relaxation effects for the different energy components. The initial (unrelaxed) situation corresponds to the frozen-orbital description of an excited t_{2g}^3 doublet (using the $^4A_{2g}$ orbitals); the final (relaxed) situation corresponds to the SCF solution for the specific doublet. The dominant components are in boxes.

In eq 6, it was shown that—for frozen orbitals—^2E_g and $^2T_{1g}$ are very nearly degenerate and that the other two energy differences are in the ratio 3/5. Since $\Delta E' \simeq \Delta E$, the same conclusions hold true at the ΔSCF level. It is not obvious how these same conclusions could be rationalized in a simple way, on the basis of the ΔSCF results alone. In this sense, the more approximate frozen-orbital calculation definitely has its merits.

A curious result from Table VIII is that the ratio 3/5 describes not only the $\Delta E'$ ratios but also the global component ratios

$$\frac{\Delta E_a'}{\Delta E_b'} \simeq \frac{\Delta T_a'}{\Delta T_b'} \simeq \frac{\Delta C_a'}{\Delta C_b'} \simeq \frac{\Delta L_a'}{\Delta L_b'} \simeq \frac{3}{5} \qquad (11)$$

If the molecule were calculated at its equilibrium geometry, the virial theorem would impose the condition $E' = -T'$ and the first part of eq 11 would automatically be satisfied. In fact, as exemplified in Table VII, E' does not quite equal $-T'$, indicating that the SCF minimum does not coincide exactly with the experimental geometry. Yet, for the four t_{2g}^3 states, the equilibrium distances will quite probably by very close together, and the sum $E' + T'$ will be of the same sign and the same order of magnitude in all cases. As a consequence $\Delta T_a'/\Delta T_b' \simeq \Delta E_a'/\Delta E_b'$, and also $\Delta V_a'/\Delta V_b' \simeq 3/5$. As for the electron–nucleus attraction terms, it can be shown[24] on the basis of the Hellmann–Feynmann theorem that $\Delta L_a'/\Delta L_b' \simeq \Delta E_a'/\Delta E_b'$, and therefore also $\Delta C_a'/\Delta C_b' \simeq 3/5$. One remarkable consequence is that

$$\frac{\Delta C_a}{\Delta C_b} \simeq \frac{\Delta C_a'}{\Delta C_b'} \qquad (12)$$

although the primed and the unprimed quantities are of opposite sign!

Somewhat similar considerations can be applied when comparing the states belonging to the $t_{2g}^2e_g^1$ configuration. If the $^4T_{2g}$ orbitals are used to describe the $^4T_{1g}$ state and if the orbitals are then allowed to relax to their optimal shape, the qualitative component shifts of Figure 5 can again be observed. But in this particular case, the C shift is not so large so as to overcompensate for the original change: the relevant C difference in Table V is 2218 + 9128 = 11 346 cm^{-1}, whereas the corresponding C' difference in Table VIII is 67 412 − 63 998 = 3414 cm^{-1}. This is quite a significant decrease, but at least $\Delta C'$ remains positive; apparently this has to do with the fact that the addition of 11 346 cm^{-1} to the $^4T_{2g}$ state represents a smaller perturbation than the addition of 20 095 or 33 502 cm^{-1} to the $^4A_{2g}$ ground state.

The relaxation effects for the interconfigurational transitions are definitely smaller than for the intraconfigurational transitions. This is due to the fact that a $t_{2g} \rightarrow e_g$ excitation modifies both the one- and the two-electron energy components, even at the frozen-orbital level (Table V). As a consequence, the induced deviation from the virial theorem is much less pronounced, and the forces restoring the proper virial ratio are smaller. Clearly, the shifts schematized in Figure 5 do not apply to this case. As a matter of fact, the frozen-orbital analysis of Table V offers a rather acceptable qualitative description of the electronic excitation act. Therefore, also at the SCF level, the reason why $^4T_{2g}$ is higher in energy than $^4A_{2g}$ (the classical $10Dq$ transition) is solely due to kinetic energy contributions; it is *not* due to potential energy effects, as migh be extrapolated from the crystal field picture. Qualitatively similar results were obtained by Wachters and Nieuwpoort[26] for the NiF_6^{4-} complexes. The conclusion that the $10Dq$ excitation essentially amounts to an increase in kinetic energy—due to a 3d-orbital contraction—might be a general feature of octahedral transition-metal complexes.

Table IX. Comparison of Certain Racah and/or Griffith Parameters for the Free Cr^{3+} Ion (Denoted by a Subscript f) and the $Cr(CN)_6^{3-}$ Complex (values in cm^{-1})

semiempirical values (first-order expressions)		SCF value (Av(d^3))	
Cr^{3+}	$Cr(CN)_6^{3-}$	Cr^{3+}	$Cr(CN)_6^{3-}$
$B_f = 980$	$B = 498$	$B_f = 1174$	$B \simeq 966^a$
$C_f = 3410$	$C = 2339$	$C_f = 4400$	$C \simeq 4084^a$
		$a_f = 195514$	$a = 173454$
		$b_f = 179894$	$b = 160062$
		$j_f = 7810$	$j = 6705$
		$e_f = 195514$	$e = 163179$
		$f_f = 8969$	$f = 7216$

[a] In MO theory, the B and C parameters for the complex cannot be given a rigorous meaning, since their definition requires a spherical symmetry; their numerical values were obtained by fitting the SCF results to the crystal field expressions.

The Nephelauxetic Effect

The Racah B and C parameters, derived from a crystal field analysis, are generally smaller than the corresponding Racah parameters of the isolated free ion. If the first-order parameters for the free ion[30] are taken to be $B_o \sim 980$ cm^{-1} and $C_o \sim 3410$ cm^{-1}, Tables I and IX show that the semiempirical nephelauxetic ratio is of the order of 0.5–0.7, indicating a very significant reduction of the free-ion values.

From a more theoretical point of view, the comparison can most easily be made with the frozen-orbital calculations. Table IX shows that the Racah B and C parameters for the free ion are rather well reproduced by the Av(d^3) SCF calculation, although the theoretical values are some 10% too high. For the Av(d^3) calculations of the complex, the Racah parameters cannot be properly defined and only the Griffith parameters have a rigorous meaning. The B and C values listed in the table are approximate values that could be obtained from an averaging process over the Griffith parameters. As a matter of fact, the numerical values of Table IX were simply obtained by fitting the SCF results to the crystal field expressions, thus

(29) The analysis in the text uses the frozen orbitals of $^4A_{2g}$, whereas Table V is based on the frozen orbitals of Av(d^3). It is also true that the relaxation energy components are strongly dependent on the orbitals one relaxes from. But this dependence very nearly disappears when one considers relaxation energy *differences*. Therefore, the discussion in the text is valid for the numbers in Table V as well.

(30) C. E. Moore, *Natl. Bur. Stand. (U.S.) Circ.*, No. 467 (1952).

yielding "theoretical" B and C values. The fact that such a fit was reasonably accurate is again related to the predominant d character of open-shell orbitals in the complex.

Clearly, the SCF calculations predict all interelectronic repulsion parameters to be smaller in the complex than in the free ion. The reasons are apparently related to the covalency of the complex, as originally invoked by Jørgensen.[31] The global reduction of the parameters may be described roughly by a factor 0.85, suggesting a significant "central-field covalency". The difference between the reduction of the a(J_{tt}) and the e(J_{ee}) parameters reflects the greater covalency of the dσ orbital ("symmetry-restricted covalency").

Qualitatively, the calculations thus reproduce the experimental finding that $\beta < 1$; but, quantitatively, the reduction factor of ~0.85 is not very satisfactory when compared to the semiempirical value of ~0.6. As stressed before, the agreement does not improve at the ΔSCF level, since the total energies hardly change upon relaxation.

Conceptually, the classical interpretation of the nephelauxetic effect can be maintained only at the frozen-orbital level of approximation: the open-shell repulsion is smaller in the more voluminous orbitals of the complex. But, at the ΔSCF level, the excitations within one given open shell do *not* correspond to an increase of the open-shell repulsion—neither in Cr^{3+} nor in the complex. In this sense, the nephelauxetic effect is only remotely connected to the open-shell repulsion.

(31) C. K. Jørgensen, "Modern Aspects of Ligand Field Theory", Elsevier, Amsterdam, New York, 1971.

Conclusions

Many features of classical crystal field theory are confirmed by detailed ab initio SCF calculations. Most notably the metal ion is found to behave more or less as an isolated entity within the complex; the open-shell orbitals are of predominant metal 3d character and are slightly antibonding with the ligands.

Conceptually, however, the crystal field picture is modified rather thoroughly at several points. More specifically, the intraconfigurational transitions from the $^4A_{2g}(t_{2g}^3)$ ground state to the excited t_{2g}^3 doublets are found to be accompanied by a *decrease* in interelectronic repulsion and an *increase* in the one-electron terms. The interconfigurational transition corresponding to the classical $10Dq$ excitation is found to correspond to a *decrease* in the potential energy and an *increase* in kinetic energy. Both conclusions are in conflict with the crystal field picture.

Numerically, the Hartree–Fock calculations are only qualitatively satisfactory; especially, the intraconfigurational transitions are calculated too high. Since the basis set used in this work is of rather high quality, the only method to improve the quantitative results would be to include extensive configuration interaction and/or the effect of the second coordination sphere.

Acknowledgment. The authors are indebted to the Belgian Government (Programmatie van het Wetenschapsbeleid) and to Prof. W. C. Nieuwpoort (R. U. Groningen) for help with the SYMOL program.

Registry No. $Cr(CN)_6^{3-}$, 14897-04-2.

Contribution from the Department of Chemistry and Biochemistry, Utah State University, UMC 03, Logan, Utah 84322

Solution Equilibria of Tertiary Phosphine Complexes of Copper(I) Halides

DENNIS J. FIFE, WILLIAM M. MOORE, and KAREN W. MORSE*

Received June 28, 1983

The solution equilibria in benzene of arylphosphine complexes of the type $L_mCu_nX_n$ (L = Ph_3P, $MePh_2P$; X = Cl, Br, I; $m:n$ = 3:1, 4:2, 3:2, 2:2, 4:4) have been investigated by using UV spectrometry and vapor pressure osmometry. The halogen appears to have only a minor effect on the dissociation. A detailed analysis of the chloride complexes shows that ligand dissociation of the L_3CuCl complexes is also accompanied by dimerization of the coordinately unsaturated copper(I) complexes through halogen bridging. However, the dimeric and tetrameric species formed by halogen bridging are found to be significant species in solution only when the ratio of L to CuCl is less than 3:1. An equilibria system is proposed with equilibrium constants derived from the modeling of the experimental data. The constants for the single ligand dissociation from $(Ph_3P)_3CuCl$ and $(MePh_2P)_3CuCl$ are 2×10^{-2} and 2×10^{-4}, respectively. With the much greater dissociation of the Ph_3P complex, the $(Ph_3P)_2CuCl$ species is the dominant form in a benzene solution made from the solid-state $(Ph_3P)_3CuCl$ complex. Solution profiles of different ratios of L to CuCl are generated to show how various species present in solution vary with concentration. The stability of the $L_mCu_nCl_n$ complexes (Ph_3P << $MePh_2P$) toward ligand dissociation is attributed to greater steric interactions of Ph_3P in comparison to $MePh_2P$.

Introduction

Detailed crystal structures have been determined for complexes of the general formula $L_mCu_nX_n$ (L = R_3P (R = alkyl or aryl); X = Cl, Br, I; $m:n$ = 3:1, 4:2, 3:2, 2:2, 4:4).[1-6] Representations of the various structures are shown in Figure 1. The complete series of structures (a–f) have not been isolated for any one given ligand. The preferred crystal structure of a given complex of this type appears to be governed by the steric size of the ligand. For bulky ligands such as triphenylphosphine or tricyclohexylphosphine, substantial intramolecular steric repulsions (R--R and R--X) have been suggested to hinder the approach of the halogen to the metal atom prohibiting effective formation of halogen bridging.[6,7]

Structural integrity is not necessarily retained when these complexes are placed in solution.[7-9] Attempts to identify and determine the relative concentrations of the various species present in the solution phase have met with little success. The formation of polynuclear species through halogen bridging in conjunction with ligand dissociation causes many experimental

(1) Jardine, F. H. *Adv. Inorg. Radiochem.* **1975**, *17*, 115.
(2) Gill, J. T.; Mayerele, J. J.; Welcker, P. S.; Lewis, D. F.; Ucko, D. A.; Barton, D. J.; Stevens, D.; Lippard, S. J. *Inorg. Chem.* **1976**, *15*, 1155.
(3) Lewis, D. F.; Lippard, S. J.; Welcker, P. S. *J. Am. Chem. Soc.* **1970**, *92*, 3805.
(4) Churchill, M. R.; Kalra, K. L. *Inorg. Chem.* **1974**, *13*, 1065.
(5) Churchill, M. R.; Rotella, F. J. *Inorg. Chem.* **1979**, *18*, 166.
(6) (a) Moers, F. G.; Op Het Veld, P. H. *J. Inorg. Nucl. Chem.* **1970**, *22*, 3225. (b) Teo, V.; Barnes, D. M. *Inorg. Nucl. Chem. Lett.* **1976**, *12*, 681.
(7) Lippard, S. J.; Mayerle, J. *Inorg. Chem.* **1972**, *11*, 753.
(8) Muetterties, E. L.; Alegranti, C. W. *J. Am. Chem. Soc.* **1970**, *92*, 4114.
(9) Abel, E. W.; McLean, R. A. M.; Sabberwal, I. H. *J. Chem. Soc. A* **1969**, 133.

0020-1669/84/1323-1684$01.50/0